Am J Physiol Heart Circ Physiol 314: H928–H939, 2018.
First published January 26, 2018; doi:10.1152/ajpheart.00602.2017.

RESEARCH ARTICLE | *Signaling and Stress Response*

Myocardial infarction-induced microRNA-enriched exosomes contribute to cardiac Nrf2 dysregulation in chronic heart failure

Changhai Tian, Lie Gao, Matthew C. Zimmerman, and Irving H. Zucker

Department of Cellular and Integrative Physiology, University of Nebraska Medical Center, Omaha, Nebraska

Submitted 11 October 2017; accepted in final form 15 January 2018

Tian C, Gao L, Zimmerman MC, Zucker IH. Myocardial infarction-induced microRNA-enriched exosomes contribute to cardiac Nrf2 dysregulation in chronic heart failure. *Am J Physiol Heart Circ Physiol* 314: H928–H939, 2018. First published January 26, 2018; doi:10.1152/ajpheart.00602.2017.—The imbalance between the synthesis of reactive oxygen species and their elimination by antioxidant defense systems results in macromolecular damage and disruption of cellular redox signaling, affecting cardiac structure and function, thus contributing to contractile dysfunction, myocardial hypertrophy, and fibrosis in chronic heart failure [chronic heart failure (CHF)]. The Kelch-like ECH-associated protein 1-nuclear factor erythroid 2-related factor 2 (Nrf2) pathway is an important antioxidant defense mechanism and is closely associated with oxidative stress-mediated cardiac remodeling in CHF. In the present study, we investigated the regulation of myocardial Nrf2 in the postmyocardial infarction (post-MI) state. Six weeks post-MI, Nrf2 protein was downregulated in the heart, resulting in a decrease of Nrf2-targeted antioxidant enzymes, whereas paradoxically the transcription of Nrf2 was increased, suggesting that translational inhibition of Nrf2 may contribute to the dysregulation in CHF. We therefore hypothesized that microRNAs may be involved in the translational repression of Nrf2 mRNA in the setting of CHF. Using quantitative real-time PCR analysis, we found that three microRNAs, including microRNA-27a, microRNA-28-3p, and microRNA-34a, were highly expressed in the left ventricle of infarcted hearts compared with other organs. Furthermore, in vitro analysis revealed that cultured cardiac myocytes and fibroblasts expressed these three microRNAs in response to TNF-α stimulation. These microRNAs were preferentially incorporated into exosomes and secreted into the extracellular space in which microRNA-enriched exosomes mediated intercellular communication and Nrf2 dysregulation. Taken together, these results suggest that increased local microRNAs induced by MI may contribute to oxidative stress by the inhibition of Nrf2 translation in CHF.

NEW & NOTEWORTHY The results of this work provide a novel mechanism mediated by microRNA-enriched exosomes, contributing to the nuclear factor erythroid 2-related factor 2 dysregulation and subsequent oxidative stress. Importantly, these new findings will provide a promising strategy to improve the therapeutic efficacy through targeting nuclear factor erythroid 2-related factor 2-related microRNAs in the chronic heart failure state, which show potentially clinical applications.

exosomal microRNAs; myocardial infarction; nuclear factor erythroid 2-related factor 2 dysregulation; oxidative stress

INTRODUCTION

Chronic heart failure (CHF) is a major cause of mortality and morbidity worldwide and is a growing public health concern due, in part, to an aging population (46). Heart failure is associated with cardiac hypertrophy and remodeling, and the pathogenesis of CHF is, in part, attributed to cardiac oxidative stress (15, 42). Increased reactive oxygen species (ROS) affects multiple biological funcitons ranging from myocyte function to excitation-contraction coupling to the regulation of coronary blood flow (1, 4, 49). An imbalance between the synthesis of free radicals and their elimination by antioxidant defense systems results in macromolecular damage and disruption of normal cellular redox signaling, thus affecting cardiac structure and function, contributing to the contractile dysfunction, myocardial hypertrophy, and fibrosis observed in CHF (7, 40, 41). Antioxidant enzymes, phase II detoxifying enzymes, and other detoxification proteins that contain antioxidant response elements (AREs) in the promoter regions of their genes are critical elements in preserving redox balance. Nuclear factor erythroid 2-related factor 2 (Nrf2) is a major regulator of these AREs. Many Nrf2-regulated enzymes have been implicated in the pathogenesis of cardiovascular diseases and are strongly associated with oxidative stress-mediated cardiac remodeling and heart failure (2, 18, 26). The Nrf2/ARE signaling pathway plays an important role in preventing oxidative cardiac cell injury in vitro (53) and protects the heart from maladaptive remodeling and cardiac dysfunction (18, 29). Thus, it is important to understand the regulation of Nrf2 in the CHF state to develop novel therapeutic strategies in the treatment of this disease. Under normal conditions, the actin-binding protein Kelch-like ECH-associated protein 1 (Keap1) retains Nrf2 in the cytoplasm and mediates proteasomal degradation of Nrf2 through the ubiquitin ligase cullin 3 (E3) system (20). In response to oxidative stress or electrophiles, Keap1 is oxidized and releases Nrf2, which translocates to the nucleus, where it binds to AREs in promoters of Nrf2 target genes, thereby activating their expression (19, 38). Recent experimental and clinical studies have shown the importance of Nrf2 and its downstream targets in the pathogenesis of cardiac remodeling and CHF induced by a number of factors including hypertension, ischemia, diabetes, and cancer therapeutics (52).

MicroRNAs are short, noncoding nucleotides regulating expression of targeted genes by mRNA degradation or translational repression. Recently, microRNAs have emerged as regulators of cell-cell communication and as paracrine signaling mediators during physiological and pathological processes (17, 48). Alterations of microRNA expression profiling has

Address for reprint requests and other correspondence: I. H. Zucker, Dept. of Cellular and Integrative Physiology, Univ. of Nebraska Medical Center, 985850 Nebraska Medical Center, Omaha, NE 68198-5850 (e-mail: izucker@unmc.edu).

been linked to cardiovascular diseases, including CHF and cardiac hypertrophy (43, 44). Some microRNAs have been directly demonstrated to be involved in blocking translation or inducing degradation of Nrf2 mRNA (23, 31, 32, 37, 51). However, the involvement of microRNAs in the posttranscriptional regulation of Nrf2 in the heart of animals with CHF remains to be elucidated. Clinical studies have shown that microRNA-27a, one of the predicted microRNAs targeting Nrf2, was significantly upregulated in the human failing heart (28). These studies suggested that microRNAs may be involved in the dysregulation of Nrf2 during the onset and progression of heart failure.

Recent studies have demonstrated that microRNAs can be actively transported by either binding to RNA-binding proteins resistant to nuclease or entrapped in exosomes to be involved in intercellular communication and signaling (47, 48). Exosomes, one of several types of cell-derived vesicles with a diameter of 30–100 nm, can serve as a novel paracrine regulator mediating intercellular communications. Cardiac fibroblast-derived microRNA-enriched exosomes mediate the cross-talk between cardiomyocytes and cardiac fibroblasts, leading to cardiomyocyte hypertrophy and contributing to heart failure (3). It is unclear if Nrf2-related microRNAs participate in the dysregulation of Nrf2 in the infarcted and failing heart. Therefore, in this study, we investigated a novel mechanism of Nrf2 dysregulation by microRNA-enriched exosomes in a rat CHF model and in a cultured cardiac cell model. We hypothesized that microRNAs regulate Nrf2 and antioxidant enzyme expression in the post-MI heart and that exosome-mediated cell communication participates in this regulation. The results demonstrate that Nrf2 protein in noninfarcted areas of the heart was downregulated at 6 wk post-MI, consistent with a decrease of Nrf2 targeting antioxidant enzymes, whereas Nrf2 mRNA levels were maintained at high levels, suggesting that post-translational regulation of Nrf2 may be involved in the progression of CHF.

MATERIALS AND METHODS

Rat model of CHF. Male Sprague-Dawley rats weighing between 320 and 410 g at the time of entry into the study were used. CHF was produced by left coronary artery ligation, as previously described by us and others (12, 24). Sham-operated (sham) rats received the same surgery but did not undergo coronary artery ligation. Six weeks after myocardial infarction (MI) or sham surgery, hemodynamics were measured in all animals by echocardiography (VEVO 2100, Visual Sonics, Toronto, ON, Canada). Rats with an ejection fraction (EF) of <40% were considered to be in CHF. Infarct size was determined postmortem by tracing the scar area and the whole left ventricle (LV) using ImageJ software [National Institutes of Health (NIH), Bethesda, MD]. The percentage of scar area to the whole LV was used to quantify infarct size. All animal experiments were approved by the Institutional Animal Care and Use Committee of the University of Nebraska Medical Center and were carried out under the guidelines of the NIH *Guide for the Care and Use of Laboratory Animals*.

Cell culture. The H9c2 cell line obtained from the American Tissue Type Collection (Manassas, VA) was cultured in DMEM supplemented with 10% FBS, 100 U/ml penicillin, and 100 μg/ml streptomycin in 75-cm^2 tissue culture flasks at 37°C in a humidified atmosphere of 5% CO_2. Cells were fed every 2–3 days and subcultured when they reached 70–80% confluence to prevent loss of differentiation. Cardiac differentiation was initiated by decreasing the percentage of serum in the media followed by retinoic acid (RA) supplementation (30); rat cardiac fibroblasts (ScienCell Research, Carlsbad, CA) were cultured with fibroblast medium-2 (Carlsbad, CA) supplemented with 2% FBS and fibroblast growth supplement-2.

Exosome purification and characterization. Exosomes were purified by sequential centrifugation as previously described (35). In brief, cells were removed from cell culture supernatants by centrifugation at 500 *g* for 10 min. To remove any possible apoptotic bodies and large cell debris, supernatants were then spun at 12,000 *g* for 20 min. Finally, exosomes were collected by spinning at 100,000 *g* for 2 h (Beckman SW40i rotor). Exosomes were washed in 10 ml PBS and pelleted again by ultracentrifugation. Exosome preparations were fixed and then spread on silicon monoxide and a nitrocellular film coated copper grid. Droplets of extracellular vesicles were removed with filter paper, air dried at room temperature, and then subjected to transmission electron microscopy (TEM, FEI Tecnai G2 Spirit TWIN, Hillsboro, OR). In addition, exosomes were lysed and subjected to Western blot analysis with the exosomal markers CD63 (H-193, Santa Cruz Biotechnology, Dallas, TX) and tumor susceptibility gene 101 protein (TSG101; 4A10, Abcam, Cambridge, MA).

MicroRNA detection in cardiac tissue and exosomes. Cardiac tissues and exosomes isolated from conditioned medium were subjected to total RNA extraction using a miRNeasy Mini Kit (QIAGEN, Germantown, MD). To allow the normalization of sample-to-sample variations in RNA isolation from exosomes, synthetic cel-microRNA-39 by Integrated DNA Technologies (Coralville, IA) was added to each denatured sample as an endogenous control. RNA was quantified using a NanoDrop spectrophotometer. Ten nanograms of total RNA were reversely transcribed using a TaqMan microRNA reverse transcription kit (Applied Biosystems, Carlsbad, CA) per the manufacturer's protocol. MicroRNA-27a, microRNA-28-3p, microRNA-34a, cel-microRNA-39, and U6 snRNA were detected using Taqman microRNA assays (Applied Biosystems) on a StepOne Real-Time PCR systems (Applied Biosystems). For all microRNAs, a threshold cycle (C_t) value of ≥40 was defined as undetectable. The $2^{-\Delta\Delta C_t}$ method was used to quantify relative microRNA expression.

In vitro tracking. Exosomes were fluorescently labeled with PKH26 Red Fluorescent Cell Linker kits (Sigma-Aldrich, St. Louis, MO) following the manufacturer's protocol with minor modifications.

Table 1. *Primer sequences used for quantitative RT-PCR (rat)*

Gene	Forward Primer	Reverse Primer
ANP	5′-ATCACCAAGGGCTTCTTCCT-3′	5′-TGTTGGACACCGCACTGTAT-3′
β-MHC	5′-TTGGCACGGACTGCGTCATC-3′	5′-GAGCCTCCAGAGTTTGCTGAAGGA-3′
Nrf2	5′-GCCAGCTGAACTCCTTAGAC-3′	5′-GATTCGTGCACAGCAGCA-3′
HO-1	5′-CGACAGCATGTCCCAGGATT-3′	5′-TCGCTCTATCTCCTCTTCCAGG-3′
NQO-1	5′-CATTCTGAAAGGCTGGTTTGA-3′	5′-CTAGCTTTGATCTGGTTGTCAG-3′
SOD2	5′-CAGACCTGCCTTACGACTATGG-3′	5′-CTCGGTGGCGTTGAGATTGTT-3′
Catalase	5′-AGCGACCAGATGAAGCAGTG-3′	5′-TCCGCTCTCTGTCAAAGTGTG-3′
GAPDH	5′-ATGATTCTACCCACGGCAAG-3′	5′-CTGGAAGATGGTGATGGGTT-3′

ANP, atrial natriuretic peptide; MHC, myosin heavy chain; Nrf2, nuclear factor erythroid 2-related factor 2; HO, heme oxygenase; NQO-1, NAD(P)H quinone dehydrogenase 1; SOD, superoxide dismutase.

In brief, exosomes were resuspended in 0.5 ml diluent C (Sigma-Aldrich). In parallel, 2 μl PKH26 dye was added to 0.5 ml diluent C and incubated with the exosome solution for 4 min with periodic mixing. To bind excess dye, 1 ml exosome-free FBS was added. Labeled exosomes were washed at 100,000 *g* for 1 h to remove excessive dye, resuspended in PBS, and then incubated with H9c2 cells in FBS-free DMEM at 37°C for various time periods. Cells were washed with PBS, fixed with 4% paraformaldehyde, and then stained with Alex Fluor 488 phalloidin (ThermoFisher Scientific,Waltham, MA) to visualize the cell skeleton as described by the manufacturer's procedure. DAPI was used for counterstaining of nuclei (blue), and fluorescent images were obtained using a Zeiss 710 Confocal Laser Scanning Microscope (Carl Zeiss, Oberkochen, Germany).

Tissue collection and Western blot analysis. Cardiac tissues were collected from the myocardial noninfarcted regions (LV free wall and septum) at 6 wk post-MI. Briefly, ~42 days after coronary ligation or sham surgery, rats were anesthetized with an intraperitoneal injection of α-chloralose (100 mg/kg) and urethane (500 mg/kg) dissolved in 2% borax solution. A remote area (noninfarcted region) of the infarcted heart was rapidly sampled and frozen in liquid nitrogen. In the sham group, myocardial samples were taken from the corresponding LV regions. All samples were homogenized with RIPA buffer (Thermo Scientific) containing a complete protease inhibitor tablet (Roche, Indianapolis, IN). Lysates were cleared by centrifugation at 14,000 *g* for 20 min. Supernatant fractions were used for Western blot analysis. Samples were separated on a 6–10% SDS-PAGE gel and transferred onto a PVDF membrane (Millipore, Billerica, MA). Membranes were blocked with 5% milk for 1 h and then incubated with primary antibodies overnight. Blots were rinsed with PBS-Tween 20 three times and then incubated with horseradish peroxidase-conjugated secondary antibodies (Thermo Scientific) for 1 h at room temperature. After being washed with PBS-Tween 20 three times, blots were applied to the chemiluminescent substrate per the manufacturer's recommendations (Thermo Scientific) and then subjected to UVP Bioimaging Systems (Upland, CA) for quantification.

Nrf2 validation by immunoprecipitation and mass spectrometry. Human embryonic kidney-293 cells cultured in DMEM with 10% FBS and 1% penicillin-streptomycin at 37°C with 5% CO_2 were

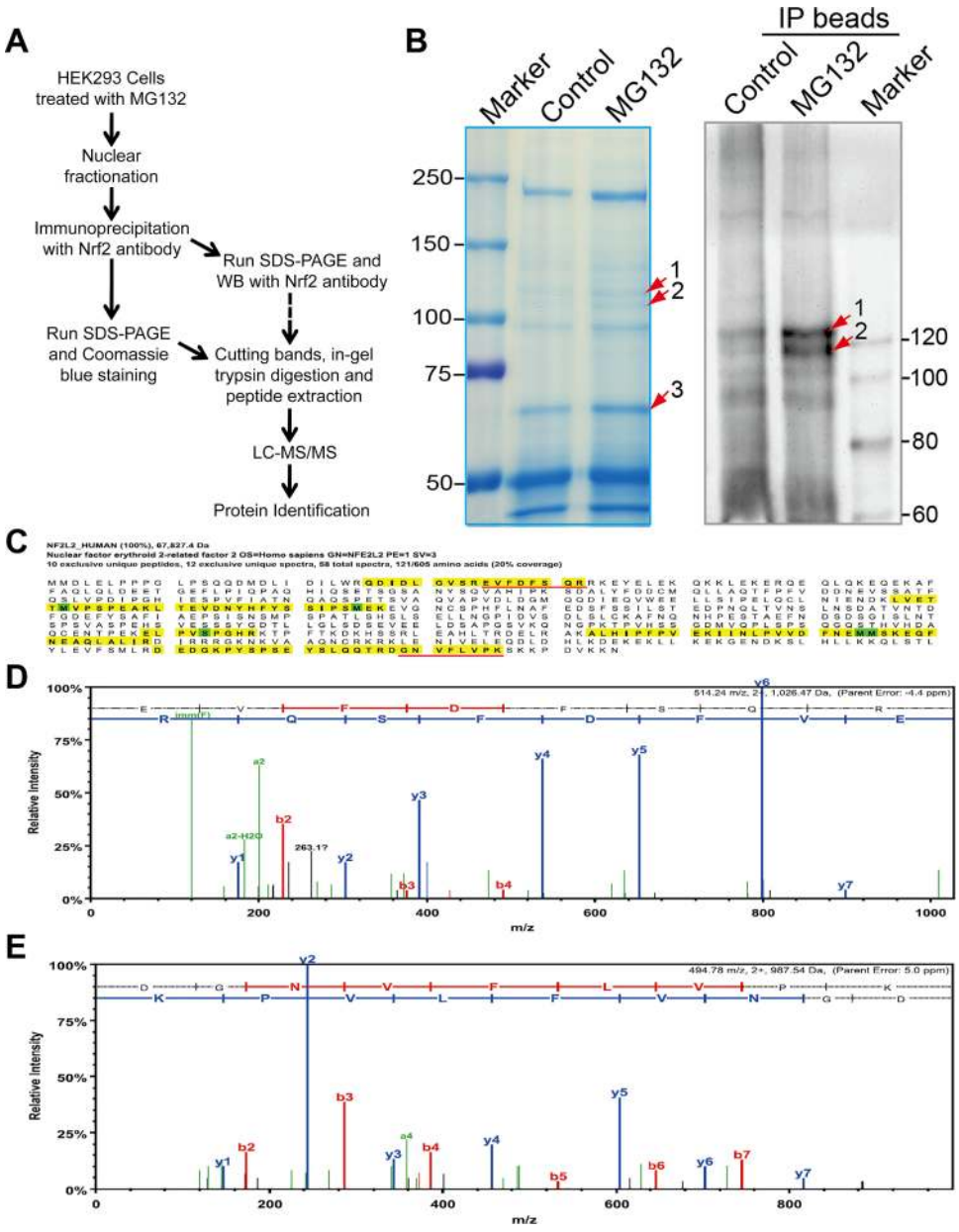

Fig. 1. Validation of nuclear factor erythroid 2-related factor 2 (Nrf2) protein by immunoprecipitation and mass spectrometry (IP-MS). *A*: diagram of the IP-MS approach to identify the Nrf2 band. *B*: human embryonic kidney-293 cells were treated with DMSO and 5 μM MG132, respectively. After 24 h of treatment, cells were collected and subjected to nuclear fractionation. Nuclear fractions were then subjected to an IP assay using anti-Nrf2 antibody (H-300) and protein A/G plus-agarose beads. The immune complex was visualized by immunoblot analysis using anti-Nrf2 antibody (H-300; *right*) and by Coomassie brilliant blue staining (*left*). Bands indicated by arrows in *B* (*left*) were cut and then subjected to in-gel trypsin digestion and subsequent MS analysis. *C*: Nrf2 coverage and representative peptide spectra obtained from MS analyses for *band 2* (*D*) and *band 1* (*E*), respectively. LC, liquid chromotography; WB, Western blot.

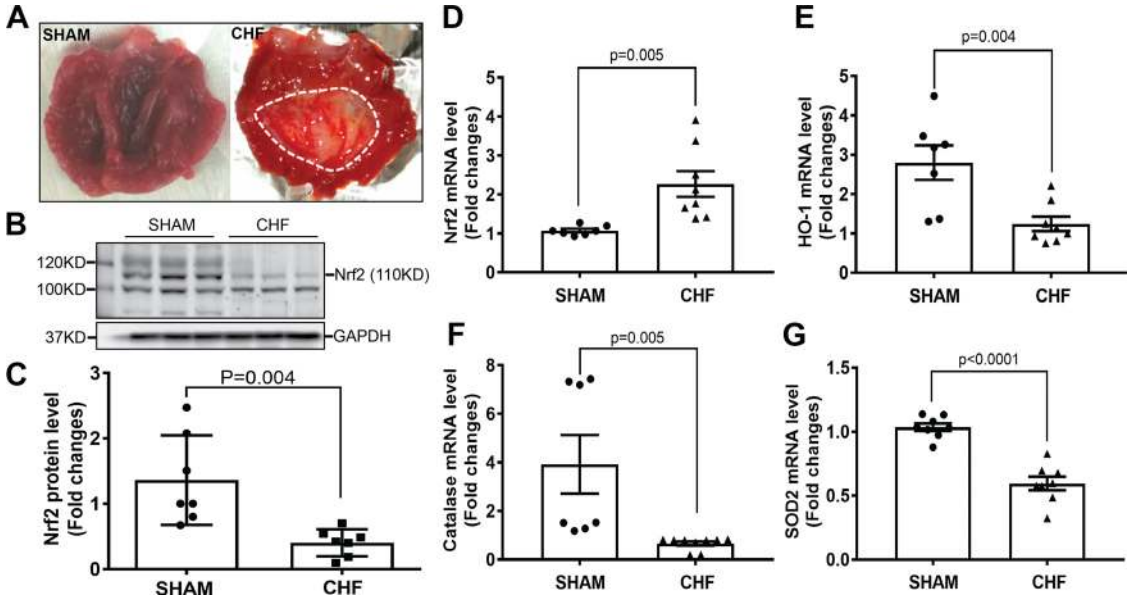

Fig. 2. Nuclear factor erythroid 2-related factor 2 (Nrf2) dysregulation is associated with chronic heart failure (CHF). *A*: example of a left ventricular infarct (dotted line) compared with a sham control heart at 6 wk after myocardial infarction. *B* and *C*: immunoblots (*B*) and pooled data (*C*) showing Nrf2 protein in the noninfarcted left ventricle (means ± SE). *D*: Nrf2 mRNA from sham and CHF left ventricles. *E*−*G*: heme oxygenase (HO)-1 (*E*), catalase (*F*), and superoxide dismutase (SOD)2 mRNA from the noninfarcted area of the left ventricle in sham and CHF rats. GAPDH was used as an internal control.

treated with 5 μM MG132, which has been demonstrated to activate the Nrf2/ARE signaling pathway in a variety of disease conditions (21, 27). After 24 h of treatment, cells were collected and subjected to nuclear fractionation using NE-PER Nuclear and Cytoplasmic Extraction Reagents (ThermoFisher Scientific) per the manufacturer's instructions. Nuclear fractions were then subjected to an immunoprecipitation assay using anti-Nrf2 antibody (H-300, sc-13032, Santa Cruz Biotechnology, Dallas, TX) and protein A/G plus-agarose beads (sc-2003, Santa Cruz Biotechnology). The immune complex was visualized by immunoblot analysis using anti-Nrf2 antibody (H-300) and by Coomassie brilliant blue staining. Based on the immunoblot image, the various bands between control and MG132-treated samples in the gel stained with Coomassie brilliant blue were cut and subjected to overnight in-gel trypsin digestion. Samples were dried in a speed vacuum and cleaned using Millipore μC18 ZipTip. Each sample was then resuspended in 0.1% formic acid and injected through an EksigentcHiPLC column (75 μm × 15 cm ChromXP C18-CL 3 μm 120 Å) onto 6600 TripleTOF (typical gradient: 2–60% acetonitrile in 60 min). The spectra obtained from mass spectrometric analyses were compared with a search in the database of Uniprot_swissprot_2015 with the use of Protein Pilot 5.0 software.

Quantitative real-time PCR. Total mRNA was isolated with TRIzol Reagent (Invitrogen, Carlsbad, CA) and RNeasy Mini Kit (QIAGEN, Valencia, CA) per manufacturer's recommendations. Reverse transcription was performed using Transcription 1st Strand cDNA Synthesis Kit (Roche, Indianapolis, IN). The quantitative RT-PCR analyses were performed using SYBR Select Master Mix (Life Technologies, Los Angeles, CA) with primer pairs (Integrated DNA Technologies) (see Table 1). The $2^{-\Delta\Delta C_t}$ method was used to quantify relative mRNA expression. GAPDH was used as an internal control. All samples were amplified in triplicate, and the mean was used for further analysis.

Transfection of microRNA mimics. H9c2 cells were cultured on six-well plates at a density of 2×10^5 cells/ml, and cell differentiation was performed in DMEM supplemented with 1% FBS plus 1 μM RA for 5 days. Differentiated cells were transfected with microRNA mimics using Xfect RNA Transfection Reagent (Clontech Laboratories, Mountain View, CA) following the manufacturer's protocol. Forty-eight hours posttransfection, Western blot analysis was performed with Nrf2 primary antibody (H-300, Santa Cruz Biotechnology). GAPDH was used as a loading control.

Transwell coculture of cardiac myocytes with fibroblasts. Rat cardiac fibroblasts were rinsed and resuspended in complete medium supplemented with 1% FBS and fibroblast growth supplement-2 at a density of 5×10^5 cells/ml, which was transferred into a transwell cell culture insert, the bottom of which comprised a membrane with a 0.4-μm pore size (Millipore). The transwell inserts containing rat cardiac fibroblasts after overnight culture were placed into the six-well culture plate containing differentiated H9c2 myocytes. The ratio of fibroblasts to myocytes was 1:1. Serum-free DMEM supplemented with TNF-α (10, 50 ng/ml) was applied to the transwell six-well plate. After 24 h of incubation, the transwell inserts were removed and cardiac fibroblasts and myocytes were collected, respectively, and subjected to Western blot analysis.

Nanoparticle tracking analysis. The size distribution of extracellular vesicles was analyzed by the NanoSight NS300 system (Malvern Instruments). Briefly, cardiac myocytes and fibroblasts were cultured in 75-cm^2 culture flasks. Extracellular vesicles were isolated from normalized volumes of serum-free culture supernatants through differential centrifugation and then resuspended with PBS. Extracellular vesicles were homogenized by vortexing followed by serial dilution of 1:1,000 in PBS and analyzed by NanoSight NS300. A blank of 0.2

Table 2. *Six-week echocardiographic data in sham and CHF rats*

Parameters	Sham	CHF
Left ventricular end-diastolic diameter, mm	7.2 ± 0.6	10.4 ± 0.6*
Left ventricular end-systolic diameter, mm	4.0 ± 0.7	8.8 ± 0.6*
Left ventricular end-diastolic volume, μl	276.2 ± 52.7	614.5 ± 83.9*
Left ventricular end-systolic volume, μl	74.6 ± 31.4	419.5 ± 67.6*
Ejection fraction, %	73.9 ± 6.8	31.9 ± 5.5*
Fractional shortening, %	44.6 ± 6.6	16.0 ± 3.0*
Infarct size, % of the left ventricle		34.2 ± 6.5

Values are means ± SE. CHF, chronic heart failure. *$P < 0.0001$ vs. the sham group.

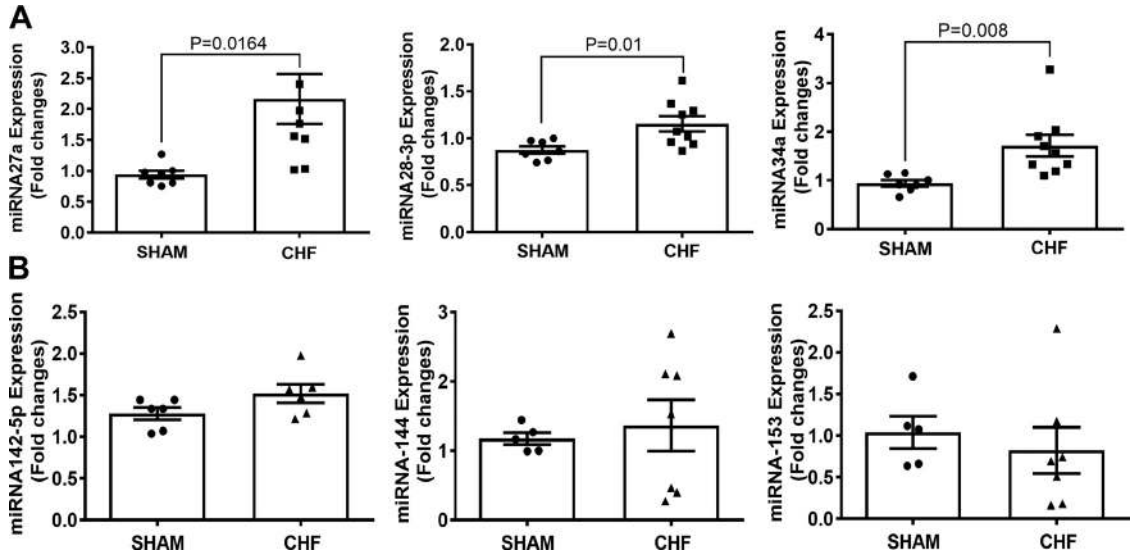

Fig. 3. Nuclear factor erythroid 2-related factor 2 (Nrf2)-related microRNAs are upregulated in the infarcted heart. Tissues from the noninfarcted area of the left ventricle were collected and subjected to RNA extraction and quantification of mature microRNAs using specific TaqMan microRNA assays, including microRNA-27a, microRNA-28a, and microRNA-34a (*A*). *B*: quantification of other mature microRNAs, including microRNA-142-5p, microRNA-144, and microRNA-153. U6 snRNA was used as an internal control (means ± SE). CHF, chronic heart failure.

μm-filtered PBS was run as a negative control. At least three analyses were done for each individual sample.

Statistical analyses. Data are reported as means ± SE. Student's *t*-tests were used to compare data between two groups (e.g., echo data, sham vs. CHF). One-way ANOVA followed by Tukey's post hoc test was used for multiple comparisons using GraphPad Prism 7.03 software. *P* values of <0.05 were considered statistically significant.

RESULTS

The Nrf2/ARE signaling pathway is dysregulated in CHF. To validate the molecular weight of Nrf2 protein detected by Nrf2 antibody (H-300) in this study, we performed immunoprecipitation and mass spectrometry as shown in Fig. 1*A* and

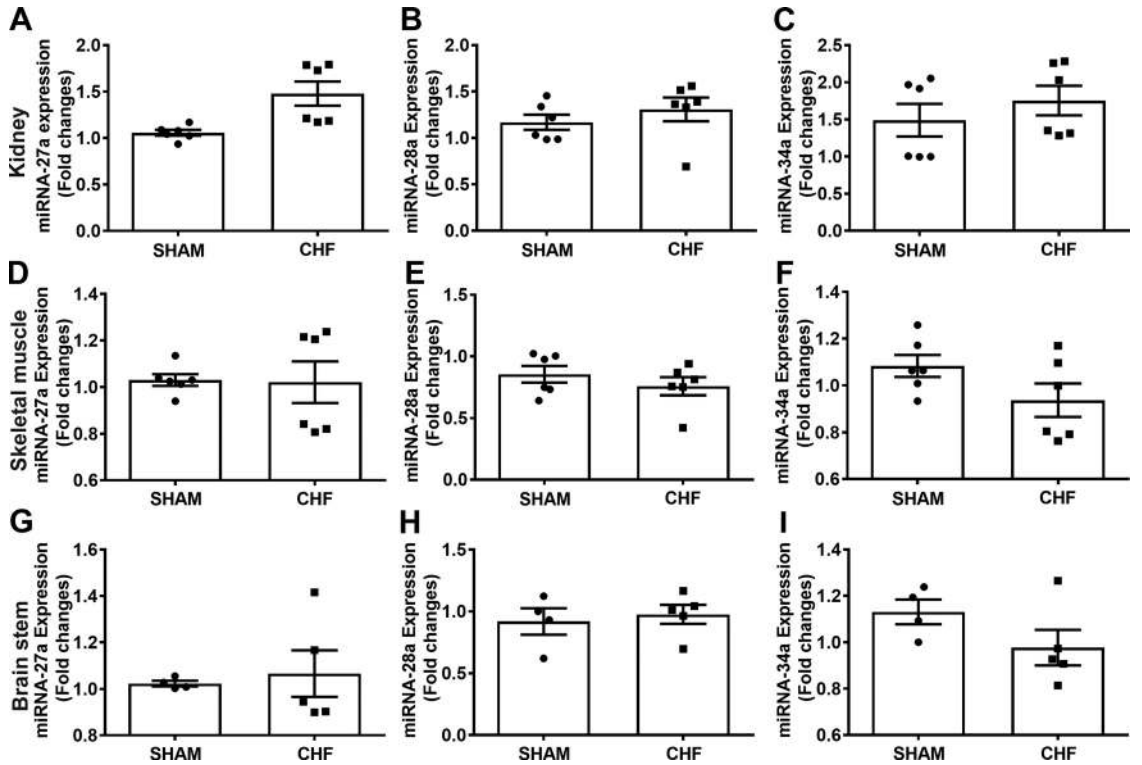

Fig. 4. nuclear factor erythroid 2-related factor 2 (Nrf2)-related microRNAs exhibit no significant changes in extra cardiac tissues. Tissues from the kidney, skeletal muscle, and whole brain stem were collected and subjected to RNA extraction and quantification of mature microRNAs using specific TaqMan microRNA assays, including microRNA-27a (*A*, *D*, and *G*), microRNA-28-3p (*B*, *E*, and *H*), and microRNA-34a (*C*, *F*, and *I*). U6 snRNA was used as an internal control (means ± SE). CHF, chronic heart failure.

observed that the band size detected by this Nrf2 antibody was similar with that in myocardial tissue (Fig. 1*B*, *right*). The bands indicated by arrows (Fig. 1*B*, *left*) were cut and subjected to in-gel digestion and then to mass spectrometry. The Nrf2 sequence coverage with digested peptides (Fig. 1*C*) and representative peptide spectra obtained from *band 1* (*bottom*) and *band 2* (*top*) are shown in Fig. 1, *D* and *E*. The database (Uniprot_swissprot_2015) searched by Protein Pilot 5.0 showed that 12 peptides from *band 2* with 95% confidence matched Nrf2 protein and had the most confident ID, suggesting that *band 2* with a molecular weight of 110 kDa could be used for Nrf2 quantification in the following experiments. Interestingly, the band at 120~130 kDa was also observed in Fig. 2*B*, which has been found in Nrf2 activator-treated cells (Fig. 1*B*, *band 1*). Further, mass spectrometry analysis also showed the band of 120~130 kDa is potentially Nrf2 protein (possibly phosphorylated; Fig. 1, *C* and *D*); however, it was not observed in all conditions. Therefore, for consistency, we only used the 110-kDa band to quantify Nrf2.

Six weeks after coronary artery ligation, rats were subjected to echocardiographic analysis. The data clearly demonstrated that LV end-diastolic diameter, LV end-systolic diameter, LV end-diastolic volume, and LV end-systolic volume were significantly increased in CHF rats compared with sham rats. On the other hand, ejection fraction and fraction shortening were significantly decreased in CHF rats. In addition, LVs exhibited an average infarct size of ~34.2% in CHF rats. All these parameters suggest classical signs of CHF (Table 2 and Fig. 2*A*). Tissues from the noninfarcted area were collected and subjected to Western blot analysis. These data demonstrate that Nrf2 protein was significantly decreased (Fig. 2, *B* and *C*) in CHF rats compared with sham rats. Interestingly, consistent with Nrf2 protein levels in the noninfarcted region of the LV, the transcription of Nrf2 target antioxidant enzymes, including heme oxygenase-1, superoxide dismutase 2, and catalase, were reduced (Fig. 2, *E*−*G*), whereas the transcription of Nrf2 was increased in CHF rats compared with sham rats (Fig. 2*D*). These observations suggest that translation of Nrf2 mRNA is repressed in the CHF state.

MicroRNAs are involved in the inhibition of Nrf2 translation. To investigate if microRNAs are involved in repression of Nrf2 translation in noninfarcted regions of the LV, we selected six microRNAs, including microRNA-27a, microRNA-28-3p (28a), microRNA-34a, microRNA-143-5p, microRNA-144, and microRNA-153, predicted to potentially bind to Nrf2 mRNA and have been directly demonstrated to be involved in blocking translation or inducing degradation of Nrf2 mRNA in cancer cells (23, 31, 32, 37, 51). Quantitative real-time PCR analysis demonstrated that microRNA-27a, microRNA-28a, and microRNA-34a were highly expressed in the myocardium of CHF animals compared with sham animals (Fig. 3*A*), whereas the expression of three other microRNAs exhibited no significant changes (Fig. 3*B*). To further determine the distribution of these microRNAs in the CHF state, we also detected the expression of three microRNAs in kidney, brain stem, and skeletal muscle of CHF rats in which Nrf2 has been reported to be either abundant (6) or important for cardiovascular function (13). The results showed that only microRNA-27a exhibited a slight increase in the kidney of CHF rats compared with selected organs relative to sham rats. MicroRNA-28a and microRNA-34a showed no obvious alterations in the three organs (Fig. 4), suggesting that microRNA expression in the CHF state may contribute to the translational inhibition of Nrf2. It has been reported that TNF-α can initiate Nrf2 activation, in part, by the generation of ROS (36). Importantly, activated Nrf2 can also regulate its own transcription through an ARE-like element located in the proximal region of its promoter (22). Consistent with these findings, our data also suggested that TNF-α promotes both transcription and translation of Nrf2 in cardiomyocytes (data not shown). To further confirm the contribution of microRNAs to Nrf2 translational repression, we transfected differentiated cardiomyocytes with microRNA-27a, microRNA-28a, and microRNA-34a mimics and then applied TNF-α to stimulate the transcription and subsequent translation of Nrf2 at 24 h posttransfection. Western blot analysis demonstrated that TNF-α-induced Nrf2 translation was significantly inhibited by microRNA mimics (Fig. 5 A, B), suggesting that local increased Nrf2-related microRNAs may contribute to Nrf2 translational inhibition.

Cardiac myocytes and fibroblasts produce and release microRNA-enriched exosomes after inflammatory stimulation. To determine whether cardiac myocytes and fibroblasts produce and secrete exosomes, cultured cardiac fibroblasts and myocytes stimulated with or without TNF-α were subjected to supernatant collection, exosome isolation by differential ultra-

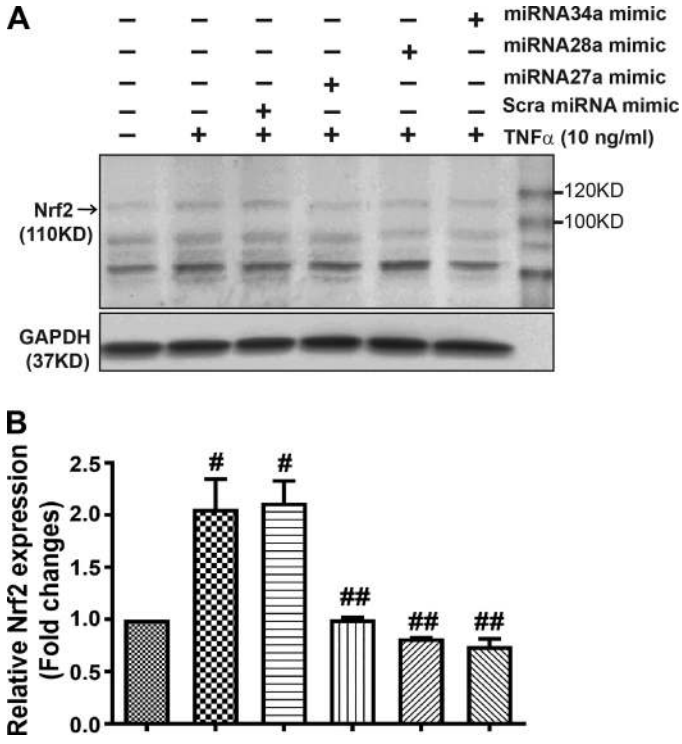

Fig. 5. TNF-α-induced nuclear factor erythroid 2-related factor 2 (Nrf2) translation was inhibited by three Nrf2-related microRNAs in cardiomyocytes. *A*: representative Western blot showing that exogenous administrations of microRNA-27a, microRNA-28a, and microRNA-34a, respectively, to cultured cardiomyocytes inhibited TNF-α-induced Nrf2 translation. *B*: data summary showing densitometry analysis of Nrf2 protein performed as normalized relative to GAPDH. Rat cardiomyocytes were transfected with a scrambled (Scra) microRNA negative control and microRNA-27a, microRNA-28a, and microRNA-34a, respectively, and then treated with or without 10 ng/ml TNF-α for 24 h. GAPDH was used as the loading control. Data are representative of three independent experiments. #$P < 0.05$ vs. control; ##$P < 0.05$ vs. Scra microRNA + TNF-α.

centrifugation, and extensive characterization, respectively. Electron microscopic analysis revealed a typical size of 30−100 nm and a characteristic cup-shaped morphology of the exosomes derived from both myocytes and fibroblasts (Fig. 6, *A*,*a* and *B*,*a*). NanoSight analysis also displayed the size distribution profiles of exosomes secreted from cultured cardiomyocytes and cardiac fibroblasts with peak diameters of 84 nm (Fig. 6*A*,*d*) and 80 nm (Fig. 6*B*,*d*), respectively. Western blot analyses further confirmed the presence of exosomal maker proteins, such as CD63 and TSG101 (Fig. 6, *A*,*b* and *c*, and *B*,*b* and *c*). Three microRNA levels in TNF-α-treated myocytes and fibroblasts were not found to be different from that in control cells (Fig. 6, *A*,*h*−*j*, and *B*,*h*−*j*). In contrast, microRNA-27a, microRNA-28a, and microRNA-34a were significantly enriched in exosomes derived from TNF-α-treated cardiac cells compared with control cells (Fig. 6, *A*,*e*−*g*, and *B*,*e*−*g*), suggesting that in response to TNF-α stimulation, two predominat cardiac cell types express microRNA-27a, microRNA-28a, and microRNA-34a, which were preferentially incorporated into exosomes and secreted into the extracellular space.

MicroRNA-enriched exosomes mediate communication between cardiac myocytes and fibroblasts, leading to Nrf2 dysregulation. Because exosomes can be derived from many cell types after MI and in CHF, further experiments were performed to test whether microRNAs are transported between cardiac fibroblasts and cardiomyocytes via exosomal transfer. We transfected cardiomyocytes with pEGFP-CD63, which is a typical exosomal marker, and then selected with G418 to enrich enhanced green fluorescent protein $(EGFP)^+$ cells (Fig. 7*A*, *top left*). Primary cardiac fibroblasts were labeled with a red fluorescent marker, PKH26, which also labels secreted exosomes (Fig. 7*A*, *top right*). PKH26-labeled fibroblasts were cultured with $EGFP^+$ cardiomyocytes and then treated with 10 ng/ml TNF-α for 24 h to stimulate exosome secretion from two type of cells. Confocal microscopy revealed that GFP^+ cardiomyocytes took up $PKH26^+$ exosomes (*i* and *ii*) and $PKH26^+$ fibroblasts took up GFP^+ exosomes (*iii*), which were distributed in the perinuclear region as indicated by the arrows (Fig. 7*A*, *bottom*). To confirm exosomal uptake by cardiomyocytes, we labeled fibroblast-secreted exosomes with PKH26 and incubated cultured cardiomyocytes with $PKH26^+$ exosomes. Analysis of exosome uptake by confocal microscopy revealed that an increased uptake of labeled exosomes was time dependent (Fig. 7*B*,*a*, *d*, and *g*) and that TNF-α stimulation promoted exosomal uptake at 24 h (Fig. 7*B*,*j*). To further confirm that exosomes are taken up into cardomyocytes and that they do not simply attach to the cell surface, we carried out three-dimensional reconstructions of the confocal image *z*-stacks, confirming the cytoplasmic localization of internalized exosomes (see Supplemental Video S1 in the Supplemental Material; Supplemental Material for this article is available at the *American Journal of Physiology-Heart and Circulatory Physiology* website).

Next, a coculture system was used to evaluate Nrf2 dysregulation mediated by exosomal crosstalk between cardiac fibroblasts and cardiomyocytes, as shown in Fig. 8*A*, where cardiac fibroblasts were not able to migrate through a 0.4-μm porous membrane filter but secreted exosomes could freely transfer. In addition, we also test whether the effects of TNF-α are dose dependent. We cocultured cardiac fibroblasts with cardiomyocytes, as shown in Fig. 8*A*, and also separately cultured two types of cells in six-well plates for 24 h in the presence of 10 and 50 ng/ml TNF-α. Western blot analysis showed that

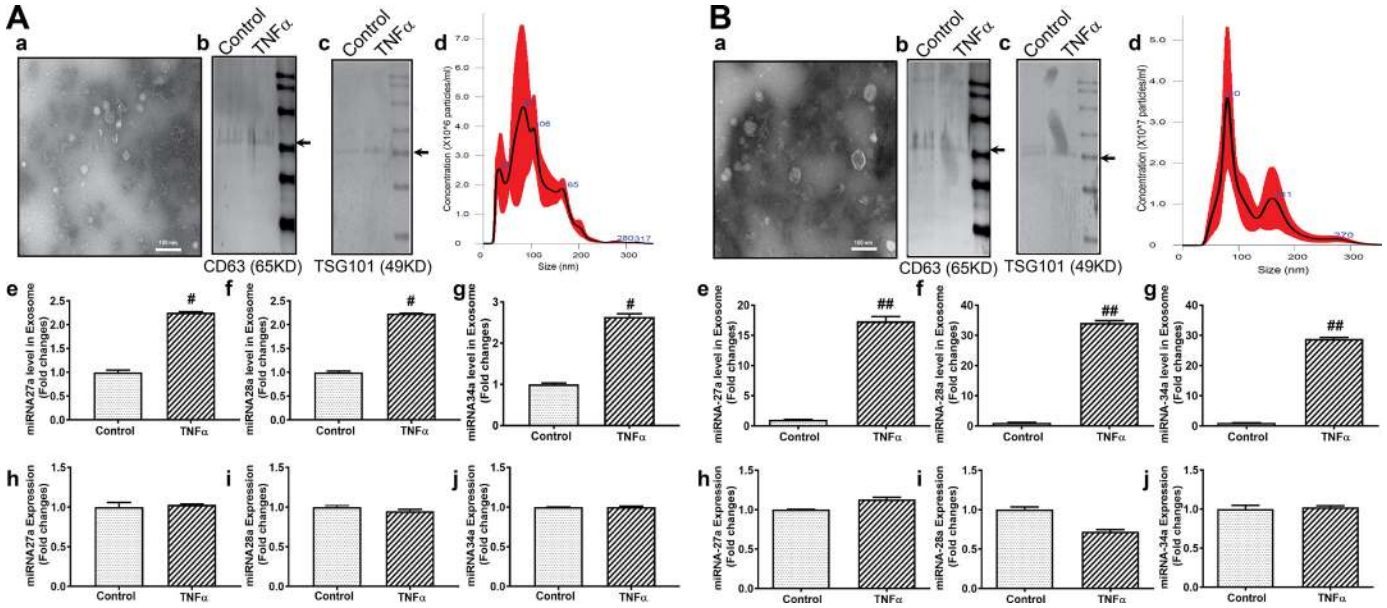

Fig. 6. Isolation and characterization of exosomes derived from cardiac cells. Exosomes isolated from conditioned medium of cardiac myocytes and fibroblasts by ultracentrifugation were fixed and then subjected to transmission electron microscopy (*A*,*a* and *B*,*a*). Exosome pellets were lysed and then subjected to Western blot analysis (10% SDS-PAGE) with CD63 and tumor susceptibility gene 101 protein (TSG101) primary antibodies (*A*,*b* and *c*, *B*,*b* and *c*). Quantitative RT-PCR results show microRNA levels in exosomes from cardiac myocytes and fibroblasts (*A*,*e*−*j*, and *B*,*e*−*j*), and Cel-microRNA-39 was used as a spike-in control. Endogenous microRNA levels in cardiac myocytes and fibroblasts are shown in *A*,*h*−*j*, and *B*,*h*−*j*, and U6 snRNA was used as an internal control. Data are representative of three independent experiments and are shown as means ± SE. # and ##$P < 0.05$ vs. control. Scale bar = 100 nm. Extracellular vesicles derived from cultured cardiomyocytes (*A*,*d*) and cardiac fibroblasts (*B*,*d*) were also subjected to a Malvern NanoSight NS300 system and analyzed by NTA 3.1 software. Five captures were collected and averaged.

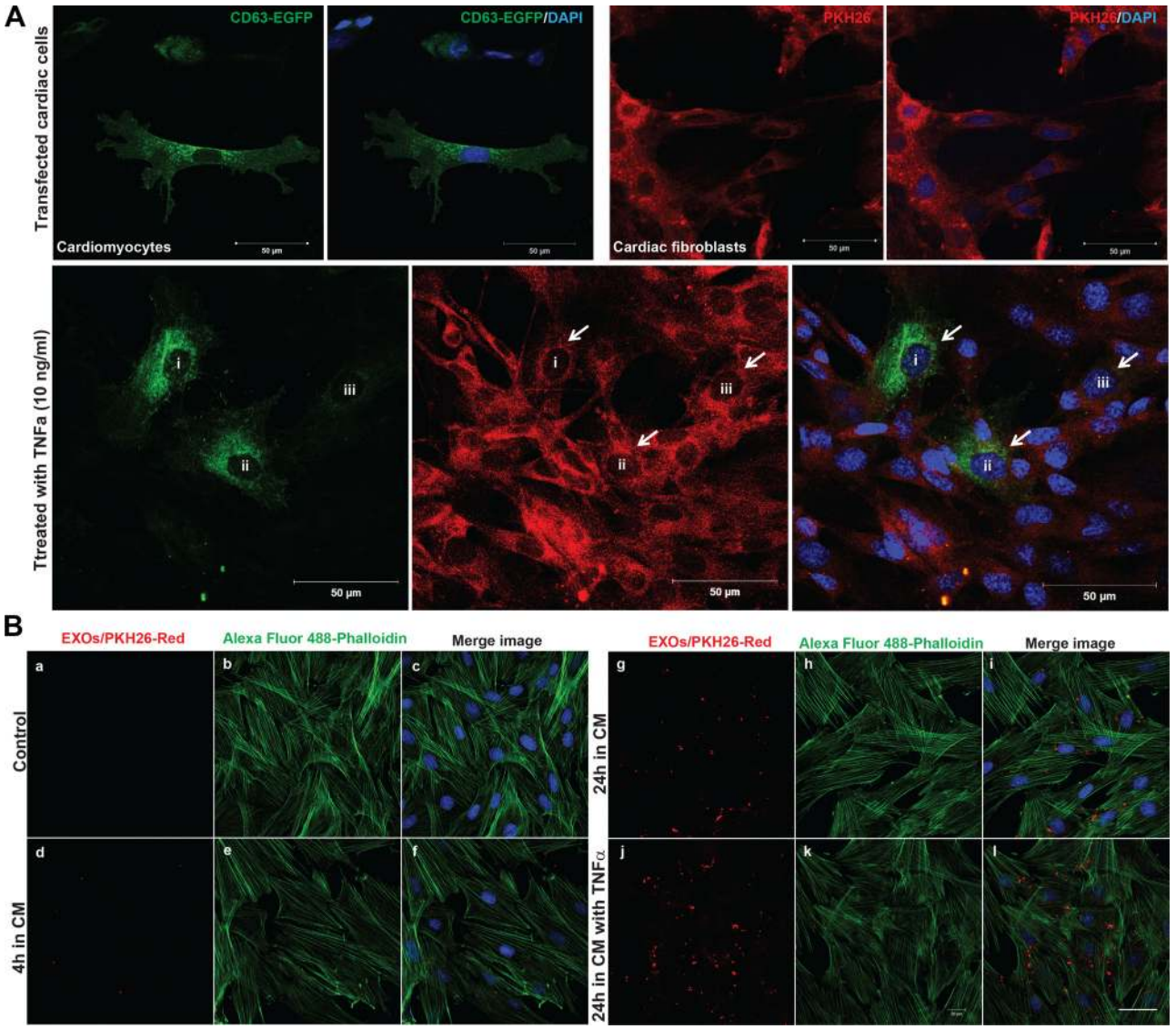

Fig. 7. Exosomes (EXOs) mediate communication between cardiac myocytes and fibroblasts, and TNF-α increase the uptake of exosomes into cardiac myocytes. *A*: cardiomyocytes transfected with pEGFP-CD63 (*top left*) and cardiac fibroblasts labeled with PKH26 red fluorescent cell linker (*top right*) were subjected to a Zeiss 710 confocal laser scanning microscope (×40 oil lens). Enhanced green fluorescent protein $(EGFP)^+$ cardiomyocytes (*i* and *ii*) and $PKH26^+$ cardiac fibroblasts (*iii*) are indicated by arrows (*A*, *bottom*). Scale bars = 50 μm. *B*: rat cardiomyocytes were incubated with PKH26-labeled exosomes (red) isolated from cardiac fibroblasts at 37°C for 4 h (*d*−*f*) and 24 h (*g*−*i*) and also incubated with exosomes and TNF-α at 37°C for 24 h (*j*−*l*). Cells were fixed and stained for confocal microscopy. Scale bar = 20 μm.

TNF-α increased Nrf2 translation when fibroblasts and cardiomyocytes were cultured separately, which was not dose dependent, whereas TNF-α-induced Nrf2 translation in cardiomyocytes and fibroblasts were repressed when cells were cocultured (Fig. 8, *B* and *C*), suggesting that secreted microRNA-enriched exosomes from cardiac cells induced by TNF-α mediate intercellular communications, leading to Nrf2 dysregulation.

Secreted microRNA-enriched exosomes from cardiac fibroblasts regulate cardiomyocyte antioxidant enzymes via dysregulation of Nrf2. To test whether the cross-talk between cardiac fibroblasts and cardiomyocytes via microRNA-enriched exosomes contributes to cardiomyocyte antioxidant enzyme regulation, we isolated exosomes from cardiac fibroblasts treated with and without TNF-α. To show that exosomal microRNA mediated Nrf2 translational inhibition, we treated cultured cardiomyocytes with 10 ng/ml TNF-α for another 24 h after we pretreated cardiomyocytes with fibroblast-derived exosomes for 24 h, as shown in Fig. 9*A*. Quantitative RT-PCR analyses demonstrated that Nrf2 transcription was increased in response to acute TNF-α stimulation (Fig. 9*B*), consistent with Nrf2 protein increases that promote the transcription of downstream targeting genes including NAD(P)H quinone dehydrogenase 1 (Fig. 9*C*) and catalase (Fig. 9*D*), and representative cardiac hypertrophy-related genes were inhibited (Fig. 9*E*, 9F). However, microRNA-enriched exosomes derived from TNF-α-treated fibroblasts not only downregulated the Nrf2/ARE signaling pathway but also promoted the expression of cardiac hypertrophy-related genes (Fig. 9, *B*–*F*), suggesting that microRNA-enriched exosomes can inhibit Nrf2 trans-

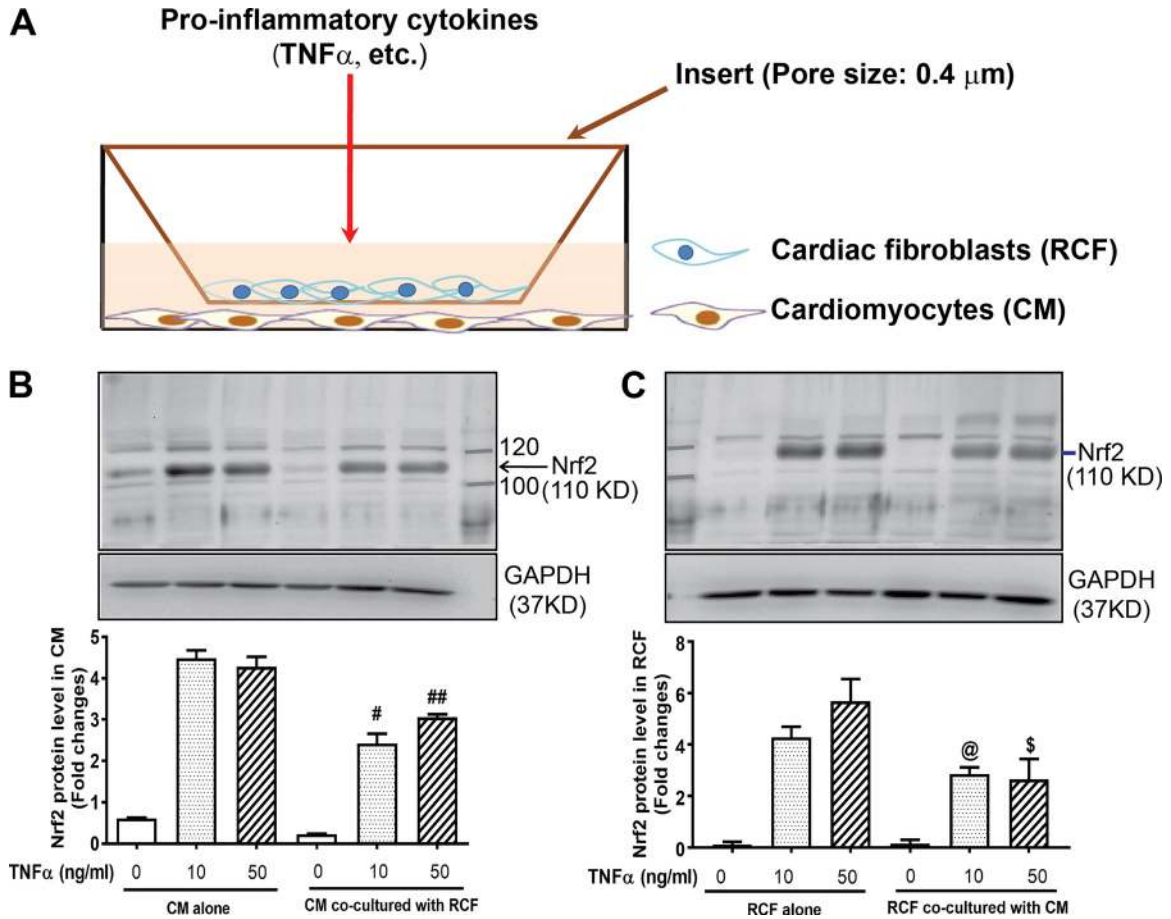

Fig. 8. Exchange of microRNA-enriched exosomes between cardiac myocytes and fibroblasts contributes to the dysregulation of nuclear factor erythroid 2-related factor 2 (Nrf2) after TNF-α stimulation. Coculture of cardiac fibroblasts cultured on Transwell cell culture inserts as well as myocytes cultured in six-well plates were performed with or without TNF-α treatment. *A*: overview of the coculture system. *B* and *C*, *top*: representative Western blots for Nrf2 expression in cardiomycytes and rat cardiac fibroblasts. (Note: both panels were split from the same gel and the size marker is duplicated). *B* and *C*, *bottom*: densitometry analysis of Nrf2 protein was performed and normalized relative to GAPDH. Data are representative of three independent experiments and are shown as means ± SE. # and ##$P < 0.05$ vs. cardiomyocytes treated with TNF-α (10 and 50 ng/ml), respectively. @ and \$$P < 0.05$ vs. cardiac fibroblasts treated with TNF-α, respectively.

lation and subsequent transcription of downstream targeting genes, contributing to cardiac hypertrophy.

DISCUSSION

In the present study, we identified a novel microRNA-enriched exosome-mediated communication between cardiac fibroblasts and cardiomyocytes, contributing to the dysregulation of the Nrf2/ARE signaling pathway and potentially leading to myocardial dysfunction. We also provided evidence for microRNA regulation of Nrf2 and antioxidant enzyme production in the post-MI and CHF states.

Increased oxidative stress along with endothelial dysfunction, inflammation, cardiac hypertrophy, and fibrosis has been implicated as contributing to the progression of CHF in both ischemic and nonischemic states (25, 39). Underlying the increased oxidative stress is an imbalance between the synthesis of oxygen free radicals and their elimination by antioxidant defense systems (5, 45). The Nrf2/ARE signaling pathway plays an important role in preventing oxidative cardiac cell injury in vitro (53) and protects the heart from maladaptive remodeling and cardiac dysfunction (18). Recently, a study from our laboratory (13) also demonstrated that *Nrf2* gene deletion in a sympathoregulatory area of the brain results in hypertension and increased sympathetic outflow as well as increased oxidative stress by impaired antioxidant enzyme expression. Therefore, it is critical for Nrf2 expression and activity to be tightly controlled. It has been well documented that Nrf2 is a substrate for the ubiquitin proteasome pathway and is negatively regulated by Keap1, a substrate adaptor for the cullin 3-Keap1-E3 ubiquitin ligase complex (19, 38) mediating Nrf2 ubiquitination and subsequent degradation under normal conditions. However, it is still unclear if Nrf2 dysregulation contributes to myocardial dysfunction in the CHF state and the mechanisms by which this dysregulation may take place. In the present study, we compared Nrf2 protein levels in the noninfarcted area of the LV from CHF and sham rats and observed that Nrf2 was significantly downregulated in CHF rats. Consistent with Nrf2 downregulation, transcription of Nrf2 downstream targeted genes was also inhibited (Fig. 2). Strikingly, and somewhat paradoxically, we found that Nrf2 transcription was increased after MI, suggesting that the translation of Nrf2 may be inhibited in the CHF state, leading to a decrease in Nrf2 protein. These observations are consistent with the presence of several short noncoding nucleotides, such

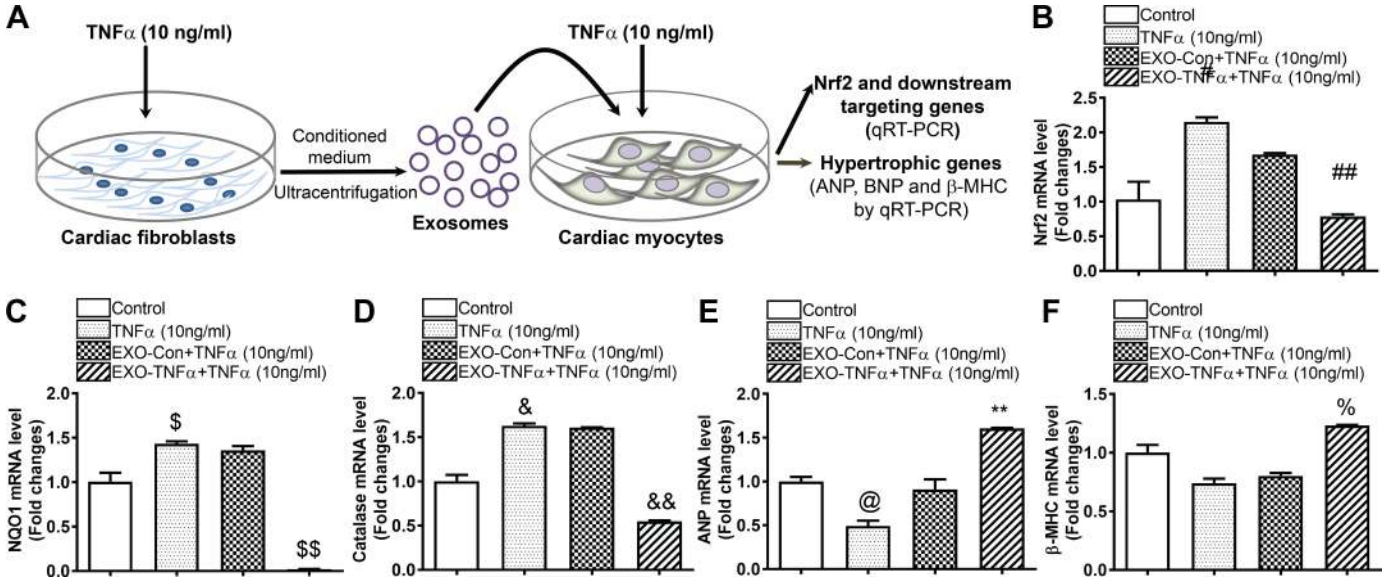

Fig. 9. In response to TNF-α stimulation, microRNA-enriched exosomes (EXOs) secreted from cardiac fibroblasts contribute to nuclear factor erythroid 2-related factor 2 (Nrf2) dysregulation and hypertrophic marker expression in cardiomyocytes. Rat cardiac fibroblasts were cultured with serum-free fibroblast medium-2 and treated with 10 ng/ml TNF-α for 24 h. Conditioned media was collected and subjected to sequential centrifugation and ultracentrifugation to purify exosomes. *A*: schematic diagram of exosome transfer experiments. Differentiated rat cardiomyocytes were pretreated with exosomes derived from either rat cardiac fibroblasts without TNF-α treatment (EXO-Con) or rat cardiac fibroblasts with TNF-α treatment (EXO-TNF-α) overnight, respectively, and then treated with 10 ng/ml TNF-α for an additional 24 h. *B*−*F*: cardiac myocytes were collected and then subjected to quantitative RT-PCR (qRT-PCR) analysis with specific primers for Nrf2 (*B*), NAD(P)H quinone dehydrogenase 1 (NQO-1; *C*), catalase (*D*), atrial natriuretic peptide (ANP; *E*), and β-myosin heavy chain (β-MHC; *F*). GAPDH was used as an internal control. Data are representative of three independent experiments and are shown as means ± SE. #, $, &, and @$P < 0.05$ vs. control; ##, $$, &&, **, and %$P < 0.05$ vs. EXO-Con + TNF-α.

as microRNAs, which are known to regulate the expression of target genes by mRNA degradation or translation repression (50). Currently, 85 microRNAs have been predicted to regulate Nrf2 mRNA, as reported in miRBase (34). Some of these microRNAs have been validated to downregulate Nrf2 expression in cancer cells, including microRNA-153, microRNA-27a, microRNA-142-5p, microRNA-144 (31, 37), microRNA-34a and microRNA-93 (23), and microRNA-28 (51). To investigate whether these microRNAs are also involved in the translational inhibition of Nrf2 mRNA in the CHF state, we examined six of them and found that three microRNAs, including microRNA-27a, microRNA-28a, and microRNA-34a, were highly expressed in noninfarcted tissue of the heart along with an increase of Nrf2 transcription (Figs. 2 and 3). Recent clinical studies have also demonstrated that microRNA-27a was increased in the failing heart (28), suggesting the potential translational repression of Nrf2 mRNA by this microRNA.

Recently, microRNA actively transported by exosomes has emerged as a novel regulator of intercellular communication and paracrine signaling during physiological and pathological processes (9, 11). In addition, cellular responses to TNF-α vary depending on the cell type and microenvironment. Nrf2 activation by TNF-α is, in part, mediated by the generation of ROS (36). Activated Nrf2 can also auto-regulate its own transcription through an ARE-like element located in the proximal region of its promoter (22), suggesting that TNF-α can regulate Nrf2 transcription and translation. Consistent with these findings, activation of transcription and translation of Nrf2 mediated by TNF-α stimulation in cardiac cells was also observed in the present study (Figs. 5, 8, and 9). Thus, we used TNF-α as either a stimulator to amplify Nrf2 transcription or an inducer to stimulate exosome secretion in this study. When we analyzed the expression of microRNA-27a, microRNA-28a, and microRNA-34a in cultured cardiac fibroblasts and cardiomyocytes treated with TNF-α, we observed that these three microRNAs were not endogenously altered. In contrast, these microRNAs were enriched in extracellular exosomes secreted from TNF-α-treated cardiac fibroblasts and cardiomyocytes, respectively (Figs. 6 and 7), suggesting a selective packaging process of microRNAs into exosomes. These findings also explain why both transcription and translation of Nrf2 were still increased in cardiac cells under TNF-α stimulation, and exogenous administrations of microRNA mimics inhibited TNF-α-induced Nrf2 translation (Fig. 5). In addition to TNF-α, we observed that other substances associated with the CHF state can also induce the secretion of microRNA-enriched exosomes from cardiac cells. These include norepinephrine, angiotensin II, and transforming growth factor-β (data not shown), suggesting that a selective packaging process of microRNAs into exosomes and preferential secretion of exosomes into the extracellular space may be a self-protective mechanism of cells under pathological conditions.

Here, we show that secreted exosomes can be transported to neighboring cells, especially under stimulated conditions (Fig. 7), and contribute to Nrf2 dysregulation (Figs. 8 and 9), which will ostensibly lead to increased oxidative stress. Increasing evidence suggests that oxidative stress is one of the molecular mechanisms and a key player involved in the development of cardiac hypertrophy (14). CHF is associated with LV hypertrophy, characterized by an increase in fetal cardiac genes, such as atrial natriuretic peptide, B-type natriuretic peptide, and β-myosin heavy chain, in response to myocardial stress (8, 10, 16). In the present study, we demonstrated that exosomes

secreted by cardiac fibroblasts after treatment with TNF-α increased expression of hypertrophic markers including atrial natriuretic peptide and β-myosin heavy chain in cultured cardiomyocytes, indicative of a cardiac hypertrophic response. However, the effects of exosomes from cardiomyocytes on cardiac fibroblasts were not addressed in this study and remain to be investigated.

There are several limitations of this study that we must acknowledge. First, as is well known, a single microRNA can target dozens to hundreds of transcripts simultaneously. In addition to targeting Nrf2, these microRNAs may also regulate other genes during cardiac development and in pathological states. For example, microRNA-27a was upregulated in hypertrophic hearts of rodents in association with β-myosin heavy chain gene upregulation by direct targeting of thyroid hormone receptor-β1 (33). Therefore, it is hard to rule out if other contributions can also be attributed to microRNA-mediated Nrf2 translational inhibition during the progression of CHF. Second, microRNA-enriched exosomes provide a novel pathway for local and distant intercellular communication. In the present study, we demonstrated the potential for local microRNA-enriched exosome-mediated Nrf2 dysregulation. However, it remains to be seen if MI-induced exosomes are released from the infarcted heart and then circulate and target the heart or other organs to exacerbate cardiac function. Finally, this study used in vitro evidence to show the potential intercellular communications in the infarcted heart, but exosomes derived from infarcted heart tissue still need to be isolated and evaluated in future studies.

In conclusion, the present study provides novel data showing that microRNA-enriched exosome-mediated intercellular communication between cardiac fibroblasts and cardiomyocytes contributes to the dysregulation of the Nrf2/ARE signaling pathway. We demonstrated that microRNA potentially targeting Nrf2 mRNA were highly expressed in the post-MI heart and abundant in exosomes released from cardiac fibroblasts, which may have the potential to communicate with cardiomyocytes. This mechanism may contribute to the downregulation of Nrf2 induced by MI and subsequent oxidative stress in CHF. These data may contribute to new strategies of therapeutic efficacy through targeting Nrf2-related microRNAs in the CHF or post-MI states.

ACKNOWLEDGMENTS

We thank Kaye L. Talbitzer, Johnnie F. Hackley, and Tara L. Rudebush for the excellent technical assistance, Dr. Guoku Hu for valuable suggestions and discussions, and Dr. Nicholas T. Woods for help with the proteomics analysis.

GRANTS

This work was supported by National Heart, Lung, and Blood Institute Grant P01-HL-62222 (to I. H. Zucker).

DISCLOSURES

No conflicts of interest, financial or otherwise, are declared by the author(s).

AUTHOR CONTRIBUTIONS

C.T. conceived and designed research; C.T., L.G., and M.C.Z. performed experiments; C.T. analyzed data; C.T., L.G., M.C.Z., and I.H.Z. interpreted results of experiments; C.T. prepared figures; C.T. drafted manuscript; C.T. and I.H.Z. edited and revised manuscript; C.T., L.G., M.C.Z., and I.H.Z. approved final version of manuscript.

REFERENCES

1. **Arcaro A, Pirozzi F, Angelini A, Chimenti C, Crotti L, Giordano C, Mancardi D, Torella D, Tocchetti CG.** Novel perspectives in redox biology and pathophysiology of failing myocytes: modulation of the intramyocardial redox milieu for therapeutic interventions—a review article from the Working Group of Cardiac Cell Biology, Italian Society of Cardiology. *Oxid Med Cell Longev* 2016: 6353469, 2016. doi:10.1155/2016/6353469.
2. **Ashrafian H, Czibik G, Bellahcene M, Aksentijević D, Smith AC, Mitchell SJ, Dodd MS, Kirwan J, Byrne JJ, Ludwig C, Isackson H, Yavari A, Støttrup NB, Contractor H, Cahill TJ, Sahgal N, Ball DR, Birkler RI, Hargreaves I, Tennant DA, Land J, Lygate CA, Johannsen M, Kharbanda RK, Neubauer S, Redwood C, de Cabo R, Ahmet I, Talan M, Günther UL, Robinson AJ, Viant MR, Pollard PJ, Tyler DJ, Watkins H.** Fumarate is cardioprotective via activation of the Nrf2 antioxidant pathway. *Cell Metab* 15: 361–371, 2012. doi:10.1016/j.cmet.2012.01.017.
3. **Bang C, Batkai S, Dangwal S, Gupta SK, Foinquinos A, Holzmann A, Just A, Remke J, Zimmer K, Zeug A, Ponimaskin E, Schmiedl A, Yin X, Mayr M, Halder R, Fischer A, Engelhardt S, Wei Y, Schober A, Fiedler J, Thum T.** Cardiac fibroblast-derived microRNA passenger strand-enriched exosomes mediate cardiomyocyte hypertrophy. *J Clin Invest* 124: 2136–2146, 2014. doi:10.1172/JCI70577.
4. **Burgoyne JR, Mongue-Din H, Eaton P, Shah AM.** Redox signaling in cardiac physiology and pathology. *Circ Res* 111: 1091–1106, 2012. doi:10.1161/CIRCRESAHA.111.255216.
5. **Canton M, Menazza S, Sheeran FL, Polverino de Laureto P, Di Lisa F, Pepe S.** Oxidation of myofibrillar proteins in human heart failure. *J Am Coll Cardiol* 57: 300–309, 2011. doi:10.1016/j.jacc.2010.06.058.
6. **Chan K, Lu R, Chang JC, Kan YW.** NRF2, a member of the NFE2 family of transcription factors, is not essential for murine erythropoiesis, growth, and development. *Proc Natl Acad Sci USA* 93: 13943–13948, 1996. doi:10.1073/pnas.93.24.13943.
7. **Costa S, Reina-Couto M, Albino-Teixeira A, Sousa T.** Statins and oxidative stress in chronic heart failure. *Rev Port Cardiol* 35: 41–57, 2016.
8. **Costello-Boerrigter LC.** Cardiac natriuretic peptides: contributors to cardiac cachexia or possible anti-obesity agents or both? *Diabetes* 61: 2403–2404, 2012. doi:10.2337/db12-0763.
9. **Das S, Halushka MK.** Extracellular vesicle microRNA transfer in cardiovascular disease. *Cardiovasc Pathol* 24: 199–206, 2015. doi:10.1016/j.carpath.2015.04.007.
10. **Ellmers LJ, Knowles JW, Kim HS, Smithies O, Maeda N, Cameron VA.** Ventricular expression of natriuretic peptides in Npr1$^{-/-}$ mice with cardiac hypertrophy and fibrosis. *Am J Physiol Heart Circ Physiol* 283: H707–H714, 2002. doi:10.1152/ajpheart.00677.2001.
11. **Emanueli C, Shearn AI, Angelini GD, Sahoo S.** Exosomes and exosomal miRNAs in cardiovascular protection and repair. *Vascul Pharmacol* 71: 24–30, 2015. doi:10.1016/j.vph.2015.02.008.
12. **Gao L, Wang WZ, Wang W, Zucker IH.** Imbalance of angiotensin type 1 receptor and angiotensin II type 2 receptor in the rostral ventrolateral medulla: potential mechanism for sympathetic overactivity in heart failure. *Hypertension* 52: 708–714, 2008. doi:10.1161/HYPERTENSIONAHA.108.116228.
13. **Gao L, Zimmerman MC, Biswal S, Zucker IH.** Selective*Nrf2* gene deletion in the rostral ventrolateral medulla evokes hypertension and sympathoexcitation in mice. *Hypertension* 69: 1198–1206, 2017. doi:10.1161/HYPERTENSIONAHA.117.09123.
14. **Gupta S, Das B, Sen S.** Cardiac hypertrophy: mechanisms and therapeutic opportunities. *Antioxid Redox Signal* 9: 623–652, 2007. doi:10.1089/ars.2007.1474.
15. **Gutierrez J, Ballinger SW, Darley-Usmar VM, Landar A.** Free radicals, mitochondria, and oxidized lipids: the emerging role in signal transduction in vascular cells. *Circ Res* 99: 924–932, 2006. doi:10.1161/01.RES.0000248212.86638.e9.
16. **Heineke J, Molkentin JD.** Regulation of cardiac hypertrophy by intracellular signalling pathways. *Nat Rev Mol Cell Biol* 7: 589–600, 2006. doi:10.1038/nrm1983.
17. **Hergenreider E, Heydt S, Tréguer K, Boettger T, Horrevoets AJ, Zeiher AM, Scheffer MP, Frangakis AS, Yin X, Mayr M, Braun T, Urbich C, Boon RA, Dimmeler S.** Atheroprotective communication between endothelial cells and smooth muscle cells through miRNAs. *Nat Cell Biol* 14: 249–256, 2012. doi:10.1038/ncb2441.

18. **Hu CM, Chen YH, Chiang MT, Chau LY.** Heme oxygenase-1 inhibits angiotensin II-induced cardiac hypertrophy in vitro and in vivo. *Circulation* 110: 309–316, 2004. doi:10.1161/01.CIR.0000135475.35758.23.
19. **Kaspar JW, Niture SK, Jaiswal AK.** Nrf2:INrf2 (Keap1) signaling in oxidative stress. *Free Radic Biol Med* 47: 1304–1309, 2009. doi:10.1016/j.freeradbiomed.2009.07.035.
20. **Kobayashi A, Kang MI, Okawa H, Ohtsuji M, Zenke Y, Chiba T, Igarashi K, Yamamoto M.** Oxidative stress sensor Keap1 functions as an adaptor for Cul3-based E3 ligase to regulate proteasomal degradation of Nrf2. *Mol Cell Biol* 24: 7130–7139, 2004. doi:10.1128/MCB.24.16.7130-7139.2004.
21. **Kraft DC, Deocaris CC, Wadhwa R, Rattan SI.** Preincubation with the proteasome inhibitor MG-132 enhances proteasome activity via the Nrf2 transcription factor in aging human skin fibroblasts. *Ann N Y Acad Sci* 1067: 420–424, 2006. doi:10.1196/annals.1354.060.
22. **Kwak MK, Itoh K, Yamamoto M, Kensler TW.** Enhanced expression of the transcription factor Nrf2 by cancer chemopreventive agents: role of antioxidant response element-like sequences in the nrf2 promoter. *Mol Cell Biol* 22: 2883–2892, 2002. doi:10.1128/MCB.22.9.2883-2892.2002.
23. **Li N, Muthusamy S, Liang R, Sarojini H, Wang E.** Increased expression of miR-34a and miR-93 in rat liver during aging, and their impact on the expression of Mgst1 and Sirt1. *Mech Ageing Dev* 132: 75–85, 2011. doi:10.1016/j.mad.2010.12.004.
24. **Liu YH, Yang XP, Nass O, Sabbah HN, Peterson E, Carretero OA.** Chronic heart failure induced by coronary artery ligation in Lewis inbred rats. *Am J Physiol* 272: H722–H727, 1997.
25. **López Farré A, Casado S.** Heart failure, redox alterations, and endothelial dysfunction. *Hypertension* 38: 1400–1405, 2001. doi:10.1161/hy1201.099612.
26. **Lu Z, Xu X, Hu X, Zhu G, Zhang P, van Deel ED, French JP, Fassett JT, Oury TD, Bache RJ, Chen Y.** Extracellular superoxide dismutase deficiency exacerbates pressure overload-induced left ventricular hypertrophy and dysfunction. *Hypertension* 51: 19–25, 2008. doi:10.1161/HYPERTENSIONAHA.107.098186.
27. **Luo ZF, Qi W, Feng B, Mu J, Zeng W, Guo YH, Pang Q, Ye ZL, Liu L, Yuan FH.** Prevention of diabetic nephropathy in rats through enhanced renal antioxidative capacity by inhibition of the proteasome. *Life Sci* 88: 512–520, 2011. doi:10.1016/j.lfs.2010.12.023.
28. **Matkovich SJ, Van Booven DJ, Youker KA, Torre-Amione G, Diwan A, Eschenbacher WH, Dorn LE, Watson MA, Margulies KB, Dorn GW II.** Reciprocal regulation of myocardial microRNAs and messenger RNA in human cardiomyopathy and reversal of the microRNA signature by biomechanical support. *Circulation* 119: 1263–1271, 2009. doi:10.1161/CIRCULATIONAHA.108.813576.
29. **Matsushima S, Kinugawa S, Ide T, Matsusaka H, Inoue N, Ohta Y, Yokota T, Sunagawa K, Tsutsui H.** Overexpression of glutathione peroxidase attenuates myocardial remodeling and preserves diastolic function in diabetic heart. *Am J Physiol Heart Circ Physiol* 291: H2237–H2245, 2006. doi:10.1152/ajpheart.00427.2006.
30. **Ménard C, Pupier S, Mornet D, Kitzmann M, Nargeot J, Lory P.** Modulation of L-type calcium channel expression during retinoic acid-induced differentiation of H9C2 cardiac cells. *J Biol Chem* 274: 29063–29070, 1999. doi:10.1074/jbc.274.41.29063.
31. **Narasimhan M, Patel D, Vedpathak D, Rathinam M, Henderson G, Mahimainathan L.** Identification of novel microRNAs in post-transcriptional control of Nrf2 expression and redox homeostasis in neuronal, SH-SY5Y cells. *PLoS One* 7: e51111, 2012. doi:10.1371/journal.pone.0051111.
32. **Narasimhan M, Riar AK, Rathinam ML, Vedpathak D, Henderson G, Mahimainathan L.** Hydrogen peroxide responsive miR153 targets Nrf2/ARE cytoprotection in paraquat induced dopaminergic neurotoxicity. *Toxicol Lett* 228: 179–191, 2014. doi:10.1016/j.toxlet.2014.05.020.
33. **Nishi H, Ono K, Horie T, Nagao K, Kinoshita M, Kuwabara Y, Watanabe S, Takaya T, Tamaki Y, Takanabe-Mori R, Wada H, Hasegawa K, Iwanaga Y, Kawamura T, Kita T, Kimura T.** MicroRNA-27a regulates beta cardiac myosin heavy chain gene expression by targeting thyroid hormone receptor beta1 in neonatal rat ventricular myocytes. *Mol Cell Biol* 31: 744–755, 2011. doi:10.1128/MCB.00581-10.
34. **Papp D, Lenti K, Módos D, Fazekas D, Dúl Z, Türei D, Földvári-Nagy L, Nussinov R, Csermely P, Korcsmáros T.** The NRF2-related interactome and regulome contain multifunctional proteins and fine-tuned autoregulatory loops. *FEBS Lett* 586: 1795–1802, 2012. doi:10.1016/j.febslet.2012.05.016.
35. **Peinado H, Alečković M, Lavotshkin S, Matei I, Costa-Silva B, Moreno-Bueno G, Hergueta-Redondo M, Williams C, García-Santos G, Ghajar C, Nitadori-Hoshino A, Hoffman C, Badal K, Garcia BA, Callahan MK, Yuan J, Martins VR, Skog J, Kaplan RN, Brady MS, Wolchok JD, Chapman PB, Kang Y, Bromberg J, Lyden D.** Melanoma exosomes educate bone marrow progenitor cells toward a pro-metastatic phenotype through MET. *Nat Med* 18: 883–891, 2012. doi:10.1038/nm.2753.
36. **Rushworth SA, Shah S, MacEwan DJ.** TNF mediates the sustained activation of Nrf2 in human monocytes. *J Immunol* 187: 702–707, 2011. doi:10.4049/jimmunol.1004117.
37. **Sangokoya C, Telen MJ, Chi JT.** microRNA miR-144 modulates oxidative stress tolerance and associates with anemia severity in sickle cell disease. *Blood* 116: 4338–4348, 2010. doi:10.1182/blood-2009-04-214817.
38. **Satoh T, Okamoto SI, Cui J, Watanabe Y, Furuta K, Suzuki M, Tohyama K, Lipton SA.** Activation of the Keap1/Nrf2 pathway for neuroprotection by electrophilic [correction of electrophillic] phase II inducers. *Proc Natl Acad Sci USA* 103: 768–773, 2006. doi:10.1073/pnas.0505723102.
39. **Seddon M, Looi YH, Shah AM.** Oxidative stress and redox signalling in cardiac hypertrophy and heart failure. *Heart* 93: 903–907, 2007. doi:10.1136/hrt.2005.068270.
40. **Siwik DA, Pagano PJ, Colucci WS.** Oxidative stress regulates collagen synthesis and matrix metalloproteinase activity in cardiac fibroblasts. *Am J Physiol Cell Physiol* 280: C53–C60, 2001. doi:10.1152/ajpcell.2001.280.1.C53.
41. **Siwik DA, Tzortzis JD, Pimental DR, Chang DL, Pagano PJ, Singh K, Sawyer DB, Colucci WS.** Inhibition of copper-zinc superoxide dismutase induces cell growth, hypertrophic phenotype, and apoptosis in neonatal rat cardiac myocytes in vitro. *Circ Res* 85: 147–153, 1999. doi:10.1161/01.RES.85.2.147.
42. **Takimoto E, Kass DA.** Role of oxidative stress in cardiac hypertrophy and remodeling. *Hypertension* 49: 241–248, 2007. doi:10.1161/01.HYP.0000254415.31362.a7.
43. **Thum T, Galuppo P, Wolf C, Fiedler J, Kneitz S, van Laake LW, Doevendans PA, Mummery CL, Borlak J, Haverich A, Gross C, Engelhardt S, Ertl G, Bauersachs J.** MicroRNAs in the human heart: a clue to fetal gene reprogramming in heart failure. *Circulation* 116: 258–267, 2007. doi:10.1161/CIRCULATIONAHA.107.687947.
44. **Thum T, Gross C, Fiedler J, Fischer T, Kissler S, Bussen M, Galuppo P, Just S, Rottbauer W, Frantz S, Castoldi M, Soutschek J, Koteliansky V, Rosenwald A, Basson MA, Licht JD, Pena JT, Rouhanifard SH, Muckenthaler MU, Tuschl T, Martin GR, Bauersachs J, Engelhardt S.** MicroRNA-21 contributes to myocardial disease by stimulating MAP kinase signalling in fibroblasts. *Nature* 456: 980–984, 2008. doi:10.1038/nature07511.
45. **Tsutsui H, Ide T, Kinugawa S.** Mitochondrial oxidative stress, DNA damage, and heart failure. *Antioxid Redox Signal* 8: 1737–1744, 2006. doi:10.1089/ars.2006.8.1737.
46. **Tsutsui H, Tsuchihashi-Makaya M, Kinugawa S, Goto D, Takeshita A; JCARE-GENERAL Investigators.** Characteristics and outcomes of patients with heart failure in general practices and hospitals. *Circ J* 71: 449–454, 2007. doi:10.1253/circj.71.449.
47. **Turchinovich A, Weiz L, Langheinz A, Burwinkel B.** Characterization of extracellular circulating microRNA. *Nucleic Acids Res* 39: 7223–7233, 2011. doi:10.1093/nar/gkr254.
48. **Valadi H, Ekström K, Bossios A, Sjöstrand M, Lee JJ, Lötvall JO.** Exosome-mediated transfer of mRNAs and microRNAs is a novel mechanism of genetic exchange between cells. *Nat Cell Biol* 9: 654–659, 2007. doi:10.1038/ncb1596.
49. **Wagenfeld L, Weiss S, Klemm M, Richard G, Zeitz O.** Vascular dysfunction in ocular blood flow regulation: impact of reactive oxygen species in an experimental setup. *Invest Ophthalmol Vis Sci* 55: 5531–5536, 2014. doi:10.1167/iovs.14-14032.
50. **Wu L, Belasco JG.** Examining the influence of microRNAs on translation efficiency and on mRNA deadenylation and decay. *Methods Enzymol* 449: 373–393, 2008. doi:10.1016/S0076-6879(08)02418-X.
51. **Yang M, Yao Y, Eades G, Zhang Y, Zhou Q.** MiR-28 regulates Nrf2 expression through a Keap1-independent mechanism. *Breast Cancer Res Treat* 129: 983–991, 2011. doi:10.1007/s10549-011-1604-1.
52. **Zhou S, Sun W, Zhang Z, Zheng Y.** The role of Nrf2-mediated pathway in cardiac remodeling and heart failure. *Oxid Med Cell Longev* 2014: 260429, 2014. doi:10.1155/2014/260429.
53. **Zhu H, Jia Z, Misra BR, Zhang L, Cao Z, Yamamoto M, Trush MA, Misra HP, Li Y.** Nuclear factor E2-related factor 2-dependent myocardiac cytoprotection against oxidative and electrophilic stress. *Cardiovasc Toxicol* 8: 71–85, 2008. doi:10.1007/s12012-008-9016-0.